Latin American Journal of Solids and Structures
www.lajss.org

Stress-based fatigue reliability analysis of the rail fastening spring clip under traffic loads

Abstract

Nowadays, the rail fastening systems play an important role for preserving the connection between the rails and sleepers in various conditions. In this paper, stress based concept is used to develop a comprehensive approach for fatigue reliability analysis of fastening spring clip. Axle load, speed and material properties are assumed to be random variables. First, track and train models are analyzed dynamically in order to achieve displacement time history of fastening spring clip. Then this displacement time history is applied to the fastening spring clip in FE software to obtain variable amplitude of stresses. Crack nucleation life is calculated by rain-flow method and Palmgren-Miner linear damage rule. First Order Reliability Method (FORM) and Monte-Carlo simulation technique are employed for the reliability index estimations. The influences of various random variables on the probability of failure are investigated by sensitivity analysis. The results show that the equivalent stress range and material parameter have significant effect on fatigue crack nucleation.

Keywords

Fastening spring clip, Fatigue crack prediction, Reliability, FORM

Saeed Mohammadzadeh[a,*]
Sodayf Ahadi[b]
Mehrdad Nouri[c]

[a,*] Assistant Professor
mohammadz@iust.ac.ir
Tel.: +98 9123184943
[b]Postgraduate Student
s.ahadi62@gmail.com
[c]Postgraduate Student
m.nouri.iust@gmail.com

[a,b,c]School of Railway Engineering, Iran University of Science and Technology, Iran.

Nomenclature

A	Material Parameter
C	Damping
D	Cumulative Damage Index
D_i	Damage Index In cycle i
e	Error Factor
E |.|	Expected Value
F(t)	Load Function
g(Z)	Limit State function
K	Stiffness
L	Random Variable Parameter of load
m	Material Parameter
M	Mass
X	Vector of random variables
N_f	Number of stress cycles to failure
n_i	Number of Cycle in stress range
N_{Total}	Number of Total Cycle
R	Random Variable Parameter of Resistance
S	Stress range
S_i	Stress Range in Cycle i
S_{re}	Equivalent Stress Range
S_{ri}	Stress rang in histogram bin
Z	Random Variable Parameter
β	Reliability Index
Δ	Critical Cumulative Damage Index
Φ^{-1}	Inverse Standard Normal Distribution

1 INTRODUCTION

A wide variety of rail fastening systems, based on the needs and conditions of the track have designed and employed in railway tracks. Spring clips normally provide a flexible connection between the rail and sleepers. They also provide a mitigation to suppress the vibrations created by the traffic impacts. Preserving the transverse slope and the track gauge in an acceptable tolerance can referred as some other roles of the spring clips (Esveld, 2001; Lichtberger, 2005). Spring clips are grouped in two classes, namely the rigid and elastic types based on the flexibility. In case of rigid types, because of the high rigidity of them, permanent deformations sometimes happen under the traffic loading and the rail connection to the sleepers failed (Lichtberger, 2005). Today, with increasing of the axial load and speeds of the passenger and freight trains, the rail fastening systems need to be able to preserve the connecting between the rails to sleepers in various harsh loading conditions (Lakusic et al., 2005).

Nowadays, Vossloh spring clips type SKL14 (Figure 1) are widely used in railway lines of different countries because of a combine advantages. These spring clips are easy for installation and maintenance and it has remarkable strength against the vertical loading. The loading of the spring clips normally includes two stages: 1) Initial pre-loading applied by the fastening bolt 2) Loading made by traffic loading. The spring clips are usually potential of fatigue damage over their lifetime caused by the vibrating random loads (Lakusic et al., 2005; European standard, 2001; Farnaghi and Bahramivahdat, 2000).

Figure 1: Vossloh spring clips-type SKL14

Reliability against fatigue and fracture failure becomes always important in case of random and cycling excitation caused by traffic loading (Tabias and Foutch, 1997; Kim et al., 2001; Lee et al., 2008; Larsson, 2006; Kwon and Frangopol, 2010). There are few technical literatures about fatigue and fracture reliability analysis in railway industries (Cremona and Lukic, 1998; Mohammadzadeh and Vahabi, 2011; Mohammadzadeh et al., 2011; Moghadam et al., 2009; Mohammadzadeh and Shayanfar, 2004). Jianxi et al. (2011) provided an approach for examining the probability of fatigue crack nucleation under random force and random material properties. Three-dimensional finite element methods (FEM) were carried out to predict rail surface and subsurface stresses under different amplitudes of wheel/rail forces. Mohammadzadeh et al. (2013) assessed fatigue crack nucleation of railhead in bolted rail joint by using FEM, response surface method and reliability analysis. Their results show that the reliability index reduced rapidly because of the low cycle fatigue regime in this area. Josefson and Ringsberg (2009) examined the risk of fatigue crack nucleation in the railhead and web in the weld zone of a rail. The fatigue crack nucleation was calculated with multi-axial fatigue criterion which proposed by Dang Van and the fatigue crack propagation was investigated Paris's law. Reviewing the technical literature existed in fatigue reliability assessment of spring clips reveals there is no published study in this area. Intensive volume of production, high consumption and importance of track safety under the traffic loading are three motivations of the present reliability assessment. In this article, a method is developed for reliability analysis of spring clips under fatigue loads by use of the S-N curve and associating Miner cumulative damage rule.

2 PROBLEM DEFINITION

The aim of this article is to develop a method for fatigue reliability analysis of Vossloh spring clips under fatigue random loading. In this paper, speed and axial load are assumed to be random variables. A finite element model of the track is programmed dynamically for obtaining the response time history of the Vossloh spring clips displacement under the simulated random traffic loading. Then the results of this analysis as input variable is fed into the Finite Element (FE) software to achieve the variable amplitude of stress in critical region. Cycle counting method is implemented over the stress-time history by using the rain-flow technique. This mentioned process repeated to achieve a reasonable probability space and based on it the stress probability distribution determined. The associating S-N curve with a supporting cumulative damage rule is employed for fatigue damage estimation.

So fatigue stresses, fatigue strength parameter, critical value of cumulative damage index and the error factor applicable in random loading are considered as random variables in the proposed fatigue reliability approach. First order reliability method (FORM) and Monte Carlo simulation (MCS) technique are employed for the reliability analysis. The influences of various random variables on the probability of failure are studied through a sensitivity analysis. General flowchart of the corresponding reliability analysis of the spring clips is schematically demonstrated in Figure 2 and 3.

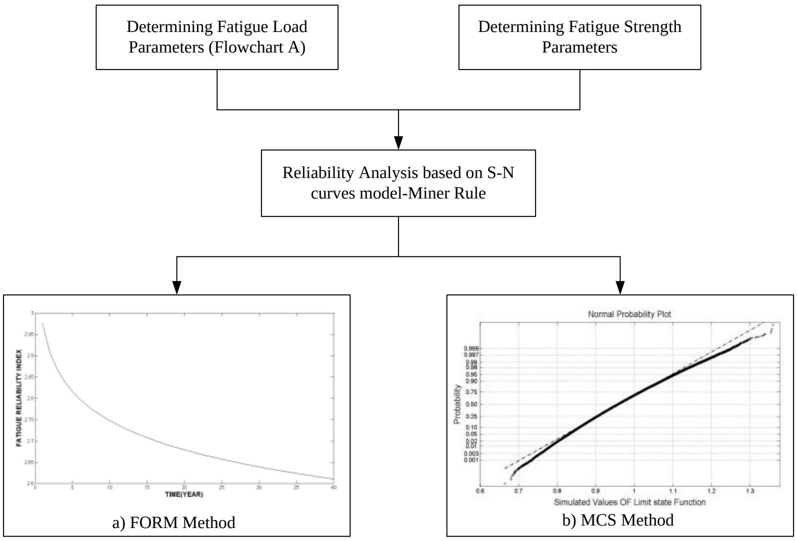

Figure 2: Flowchart of determination the reliability index using: (a) FORM (b) Monte Carlo

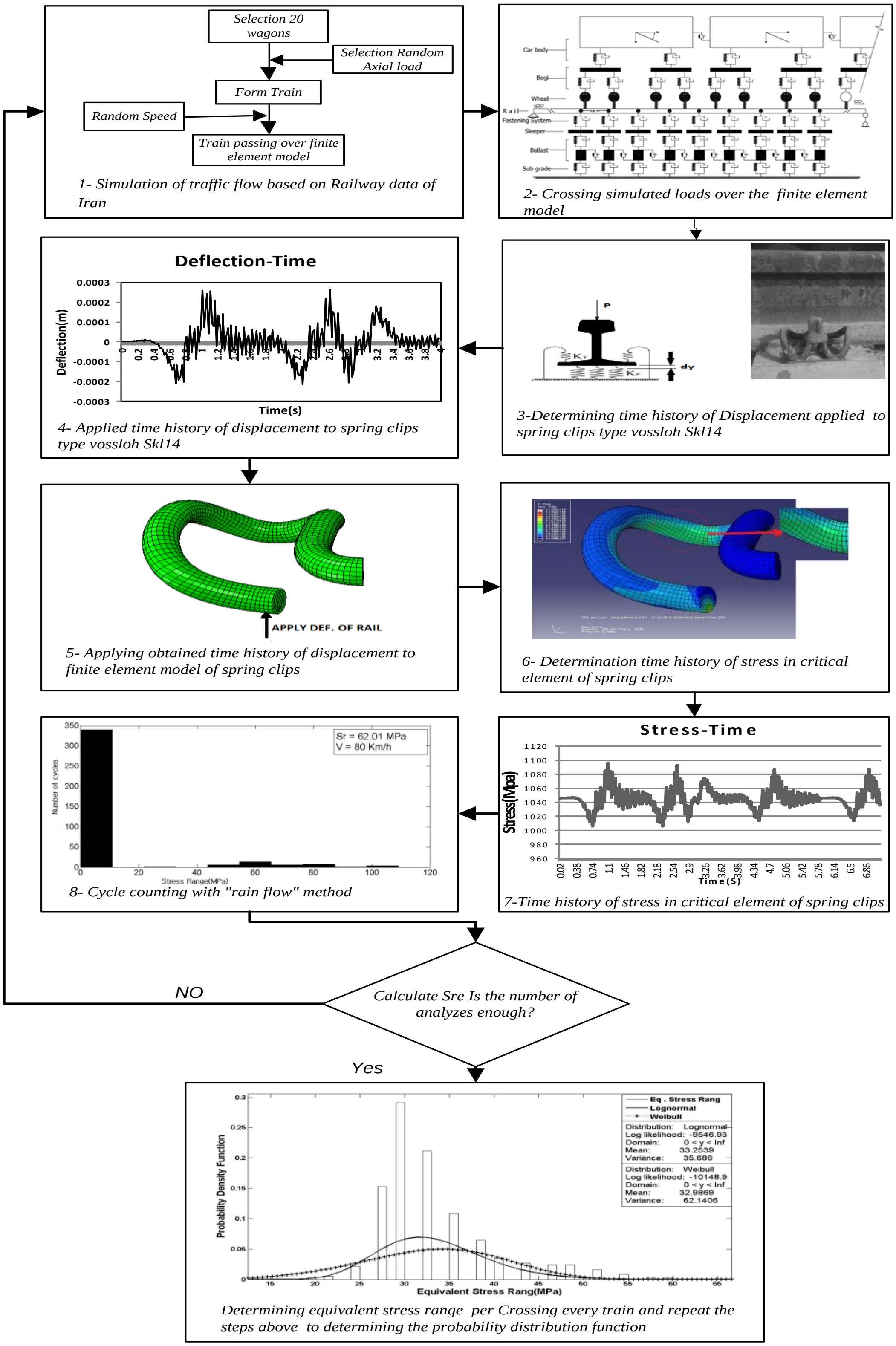

Figure 3: Flowchart of fatigue Reliability analysis of the spring clips

3 NUMERICAL ANALYSIS OF SPRING CLIP TYPE VOSSLOH SKL14

3.1 Specifications of the track and the train

SKL14 Vossloh spring clips are widely used in railroads of Iran. Therefore, fatigue reliability analysis of this spring clips is targeted in this paper. Five different steps of proposed method include are: 1) simulation of traffic loads; 2) dynamic analysis of FEM of track under simulated loads; 3) FEM analysis of the spring clips type Vossloh SKL14; 4) cycle counting and determination of distribution function of equivalent stress range; 5) reliability analysis. The main variables which substantially affect the stress values in spring clips can be referred as: 1) train speed; 2) axial load; 3) number of car-bodies; 4) roughness of the rail and wheel; 5) ballast stiffness. In this study both the speed and axial load of the train were assumed to be two random variables. For that purpose, Numerical simulation is carried out using the Monte Carlo technique (Wysokowski, 2005; Chotichai and Kanchanalal, 2006). In this paper the probability distribution of the speed and axial load was obtained in stations Arzhang-Andymeshk (South-west Iran) (Mohammadzadeh and Ghahremani, 2012). Then different trains with 20 car-bodies were selected and axial loads of each wheel set determined as a random value based on the relevant distribution function. So the train speed was randomly assigned based on the associating probability distribution. The specifications of probability distribution of these variables are listed in Table 1.

Table 1: Probability distribution of speed and axial load in stations Arzhang-Andymeshk

Random variable	Probability Distribution	Mean	Standard Deviation
Speed(m/s)	Normal	14.09	2.53
Axial load(kg)	Lognormal	22500	3750

In this paper, the length of track model was 48 m and the numbers of nodes according to the sleeper intervals (0.6 m) were set to be 81. Mechanical specifications of the different components of the track and train are listed in Table 2 and 3 respectively (Zakeri et al., 2009). A train with 20 car-bodies is selected and the corresponding axial load (the mass of wagon) was randomly assigned. At the next stage the speed of train is randomly assigned. By analyzing the FEM under random loads, time histories of displacement of spring clips eventually gained.

Table 2: Mechanical specification of the track model

Parameters of Track	**Quantities**	**Unit**
Rail mass per unit length (M_r)	60	kg/m
Mass of sleeper (M_s)	320	kg
Mass of each block of ballast under sleeper (M_b)	1300	kg
Elasticity modulus of rail (E)	206000000	kN/m^2
Moment of inertia of rail (I)	0.0000322	m^4
Distance between sleepers(a)	0.6	m
Stiffness of pad (between the rail and sleeper) (K_p)	240000	kN/m
Stiffness of ballast (between the sleeper and ballast) (K_b)	70000	kN/m
Stiffness of sub grade (between the ballast and sub grade) (K_f)	120000	kN/m
Damping of ballast (between sleeper and ballast) (C_b)	170	kN.s/m
Damping of sub grade (between ballast and sub grade) (C_f)	60	kN.s/m
Damping of pad (between rail and sleeper) (C_p)	230	kN.s/m
Cross section of rail (A_{Rail})	0.0077	m^2

Table 3: Mechanical specification of the train model

Parameters of Train	Quantities	Unit
Poisson's ratio (ν)	0.3	-
Yield stress (f_y)	1300	MPa
Total mass of wagon (M_c)	49500*	kg
Total mass of bogies (M_t)	10750	kg
Wheel mass (M_w)	2200	kg
Moment of inertia(wagon) (J_c)	1700000	kg.m^2
Moment of inertia (bogies) (J_t)	9600	kg.m^2
Half distance between axis of bogies (L_c)	9.5	m
Half distance between wheels of bogies (L_t)	1.25	m
Stiffness of bogies (between bogies and wagons) (K_t)	1720	kN/m
Stiffness of wheel (between wheel and bogies) (K_w)	4360	kN/m
Damping of bogie (between bogie and wagon) (C_t)	300	kN.s/m
Damping of wheel (between wheel and bogie) (C_w)	220	kN.s/m

*This quantity assigned based on axial load probability properties in table (1)

3.2 Dynamic simulation between the track and the train

Dynamic analysis of track and train has studied by many researchers. For this purpose, various models of track and rail vehicle have been developed (Xia et al., 2007; Younesian and Kargarnovin, 2009; Younesian et al., 2005; Kargarnovin et al., 2005; Younesian et al., 2006; Zakeri and Xia 2008, 2009; Zakeri et al., 2009). In this article a dynamic analysis model for train and track couple system have developed to obtain the time history of displacement of spring clips (Figure 4). Because of symmetrical of track and train, only one half of the coupled system considered for reducing time consuming. The flow chart of this process is shown in Figure 5. As can see, the dynamic analysis model includes of two parts train model and track model. First the specifications of track and train determined. In the next matrixes of mass, damping and stiffness of components of couple system formed and this followed by bumble and formed overall matrix of system.

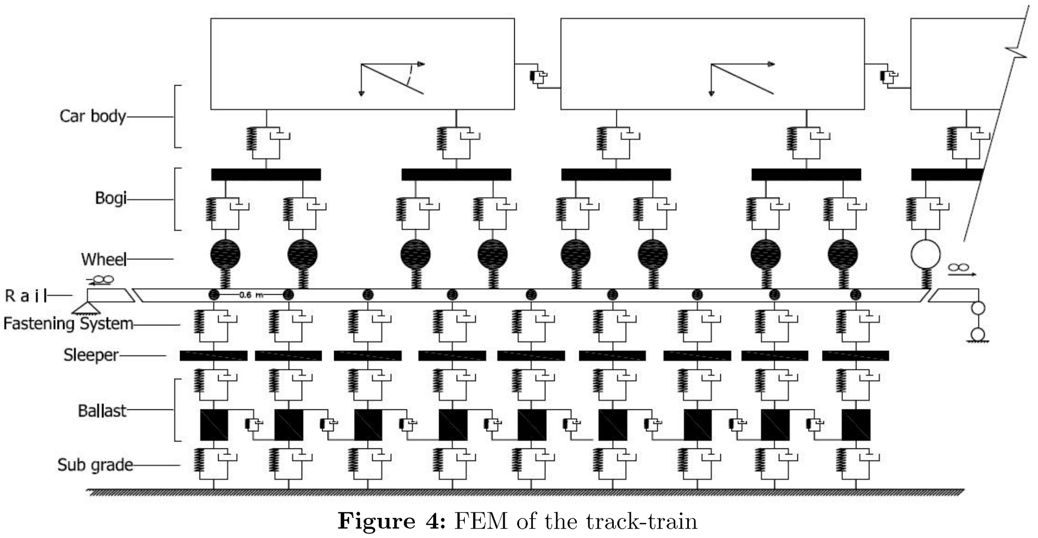

Figure 4: FEM of the track-train

The car body, bogies and wheel sets of train are assumed rigid. The vehicle is modeled with ten degree of freedom including the car body mass and its moment inertia, two bogies masses and their moment of inertia and four wheel sets and spring masses. For vehicle body, the equations of the vertical deflection and pitching motions of the lumped masses described using second order ordinary differential equations in the time domain.

A typical ballasted track is used to dynamic analysis. For this purpose, finite element model of track has been developed. The subsystem is illustrated in Figure 5. As shown, it is included rail, fastening system, ballast and subgrade. The assumption that used in the modeling of track components is described as following.

Rail is considered as an Euler-Bernoulli beam that divided into finite segments. The semi-infinite boundary elements are considered in the both end. Every segment has two degree of freedom in vertical motion. The matrixes of mass, stiffness, damping are conducted by using direct stiffness method. The fastening system is consisted of rail pad and spring clips. The load–deflection behaviors of them are considered linear and modeled by spring and damper in parallel. In this study, the sleeper is modeled by a centralized mass in joint point that connected to vicinity elements with spring and damper. Ballast and subgrade are modeled as additional masses below each sleeper; it is interconnected by spring and damper in shear. In this article, the wheel-rail contact is modeled by a nonlinear Hertzian spring. Accordingly, the corresponding mass matrix, stiffness and damping matrixes are assembled (see Appendix (A)).

In this paper, Newmark method is used to solve differential equation (Bathe, 1996; Zienkiewicz, 1977; Sun and Dhanasekar, 2002). The model has been verified by measurements that taken by Newton and Clark (1979). As shown in Figure 5, the results of model have good agreement with measurements.

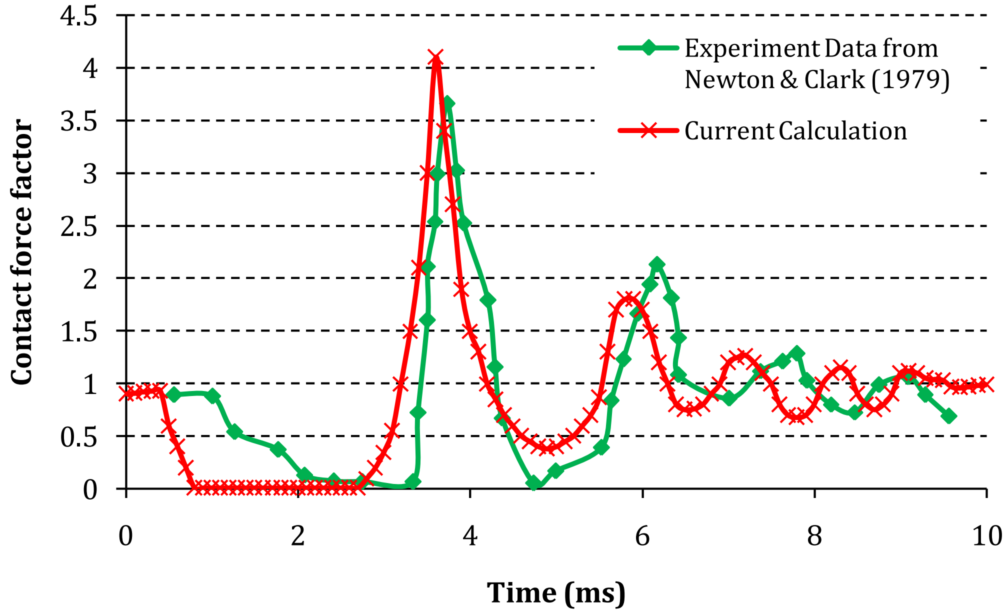

Figure 5: Comparison contact force factor between FEM results and experimental measurements

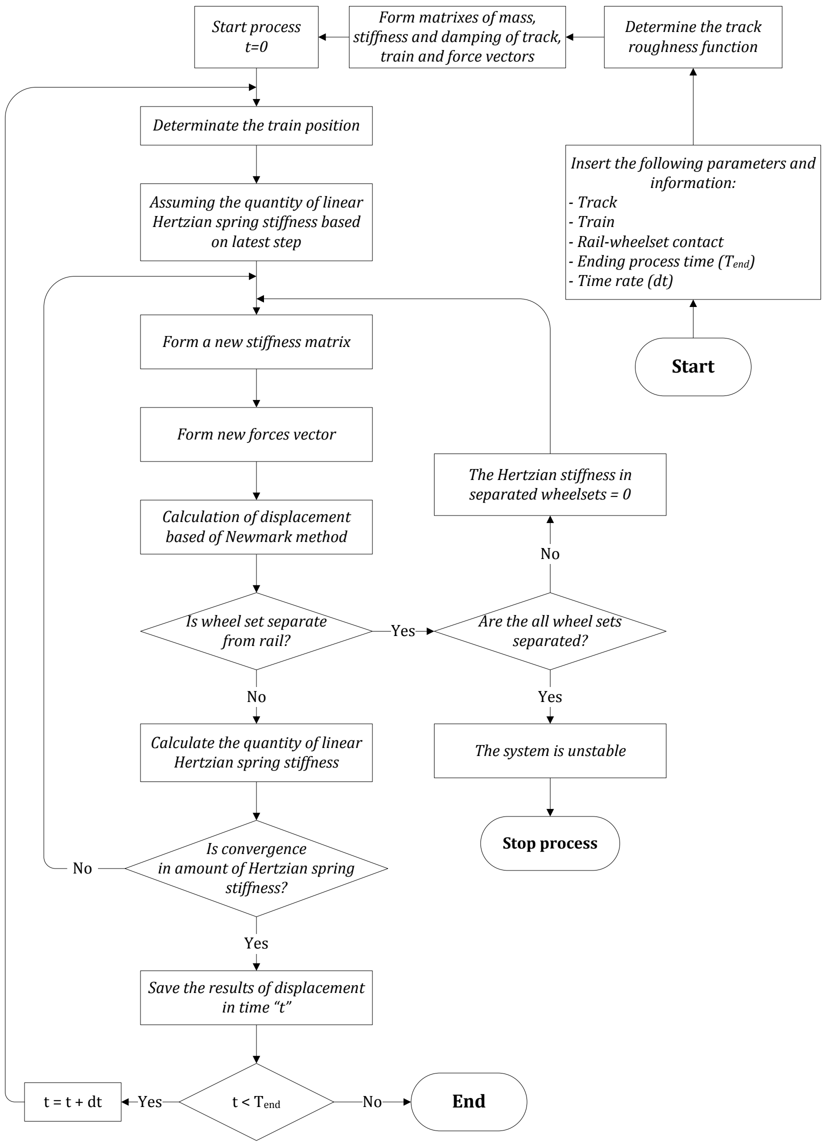

Figure 6: Flowchart of dynamic analysis of the track–train

FEM of the track was analyzed under the simulated traffic loads. For do this, in every analysis (Figure 5) the velocity and mass of car body were assigned randomly based on their probability properties. The time history of displacement of the spring clips was gained for over 3000 number of different trains.

3.3 FEM analysis of the spring clip type Vossloh SKL14

The purpose of FEM analyses was to found the maximal stress places for the SKL14 when it was set up and used. This places where volunteer to fatigue crack nucleation. FEM analysis of the SKL14 include two steps: 1) application of preloading exerted by the fastening bolts 2) displacement caused by passing traffic loads. For modeling, a typical SKL14 spring clip was three dimensionally scanned using a CMM scanning and then analyzed in ABAQUS software. To achieve reasonable results, FEM meshed finely with 5488 elements (type C3D8R) and 6780 nodes. The constants of S-N curveinclude $A_{specimen}$=6.95e71 and $m_{specimen}$=22.27 are gained by R. Moore test.

The results of these tests have been quantified as modification factor which are applied on the base line S-N data (Bannantine et al. 1990). In this article, the effect of size, types of loading and surface finish are considered as modification factor. The material properties of the spring clips type SKL14 are shown in Table 4. The results of FEM were validated by results of force-displacement experiment (Figure 7). So seven sample of SKL14 was used in this experiment. The selected samples were loaded in five steps by displacement 4.7, 6.4, 8, 9 and 11mm and corresponding load was determined in every step. To gain acceptable results, the experiment was repeated six times for each specimen and the mean value of load was used in the curve. In following the FEM also loaded under above steps and compared with experimental results. As shown in Figure 8, the force-displacement curve of FEM has good matches with outcomes of experiment.

Table 4: Mechanical specification of spring clips type SKL14

Parameter	value
Ultimate stress "S_u"	1370 (MPa)
Fatigue Limit Stress "S_{re}"	685 (MPa)
Fatigue constant (X_2) "$A_{Spring\ clip}$"	2.33e30 (MPa)
Fatigue constant "$m_{spring\ clip}$"	11.7

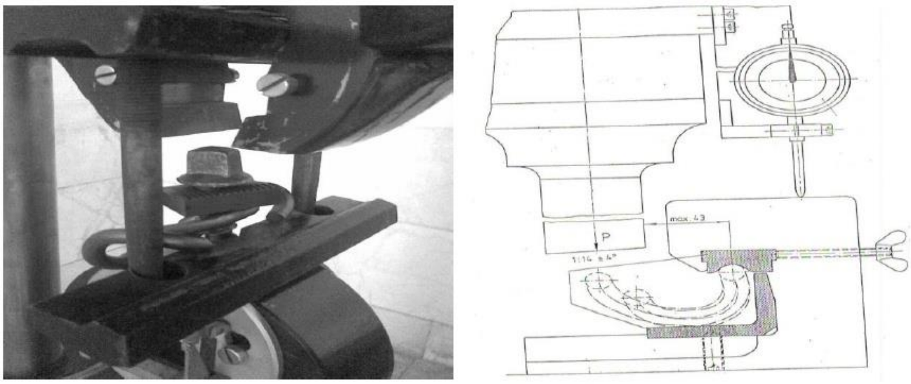

Figure 7: Force-displacement test devices

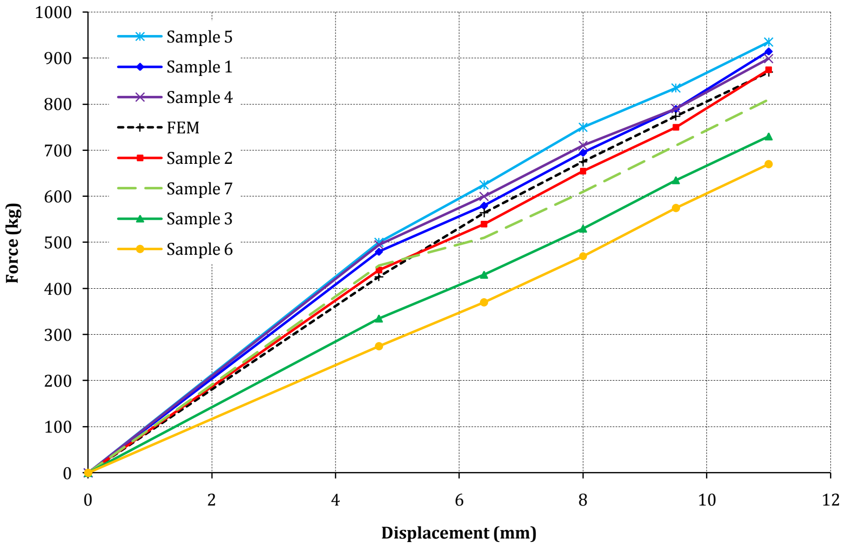

Figure 8: Validation of FEM of SKL14 by force-displacement experiment

The calibrated FEM was analyzed under time histories of displacement of FEM of track. According to the experimental results, fastening bolts produce pre-displacement of 10.5 mm in spring clips. Therefore at the first stage, a displacement of 10.5 mm was applied to FEM of SKL14 as the pre-stress condition. At the second stage, the obtained time history of displacement (results of dynamic analysis) was applied. First step, an elastic-plastic analysis was performed. In some cases found that in little number of elements the stress was exceeded yield stress. Since frequency (the number of cycles that some elements exceeding yield stress to the total number) exceeding the yield stress was low less than 0.01% (Kwon and Frangopol, 2010). Then the effect of plasticity was neglected and S-N curves model associate with miner law was used to estimating fatigue damages. The critical stress region was determined at the FEM of SKL14 and the stress time history of this region was obtained. The results of pre-stress analysis and the traffic loading analysis are shown in Figure 9.

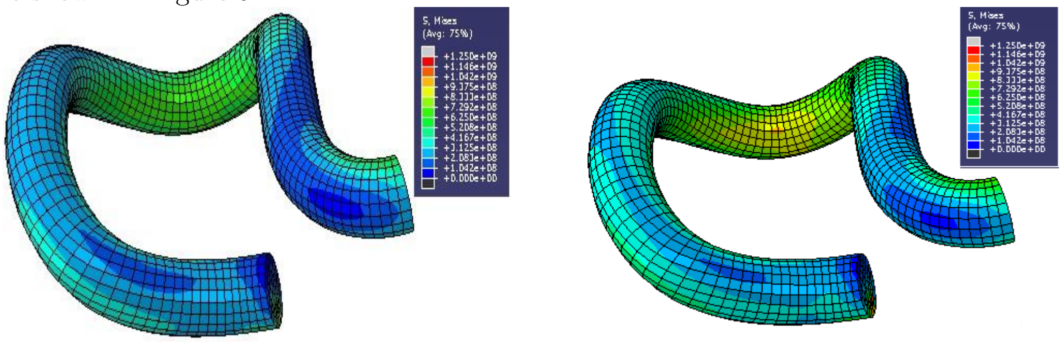

(a) (b)

Figure 9: Stress analysis of the SKL14 spring clips (a) First stage (b) Second stage

4 FATIGUE RELIABILITY ANALYSIS

4.1 Application of stress based concept to reliability analysis

Reliability analysis of structural members or systems determined if the probability level exceeds a certain value in an operational load case (NGI, 2005; Baecher and Christian, 2003; Nowak and Collins, 2000; Choi et al., 2007; Bannantine et al., 1990). If the random parameters match with the loading and resistance represented by L and R respectively then the limit state function can be expressed by:

$$g(Z) = R - L \tag{1}$$

The limit state function indicates the boundaries between the safety and failure modes of operation. According to definition of the limit state function, the probability failure is defined by equation (2). In this equation, g(Z) represents the probability distribution function of variables. Reliability index (β) can be then written as:

$$P(f) = P(g(Z) < 0) \tag{2}$$

$$\beta = -\Phi^{-1}(P(f)) \tag{3}$$

Where Φ^{-1} represents the inverse standard normal distribution function (CDF). In this study, the limit state function is formed by stress based concept in order to evaluate the probabilistic analysis of fatigue life under random loading. Since the amplitude and frequency of stresses obtained from FEM analysis is random variable, the equivalent constant amplitude stress range is used by using Miner‘s rule to estimation of fatigue damage. The stress range bin histogram data (Figure 2) are collected by Rain flow method counting method from results of FEM analysis of spring clip (Cremona et al., 2007; Stephens et al., 2001). A supporting computer program has been developed using the MATLAB software based on the ASTM 1049 code. The associating cycle counting was carried out and the equivalent stress range was calculated for the each load case by using formula 11. No doubt to find out the probability distribution function, the probability space should be as extensive as possible. The probability space contains 3000 simulations for 3000 running of different trains with different axle loads and speeds. The corresponding equivalent stress range histogram was eventually obtained using the Weibull and lognormal probability distribution function as shown in Figure 10.

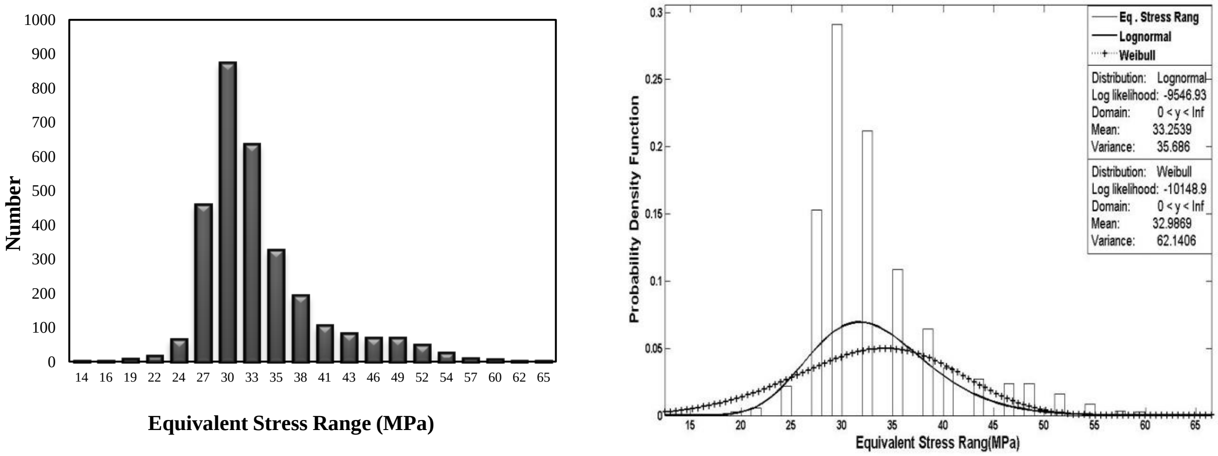

(a) (b)

Figure 10: (a) Histogram of equivalent stress range (b) fitting process with probability distribution functions

In this study, Basquin's relation is used for prediction of fatigue life. This relation states the log-log straight line relationship between the stress range under constant amplitude loading and number of stress cycles to failure which expressed as (Siddiqui and Ahmad, 2001):

$$A = N_f S^m \tag{4}$$

Where N_f is the number of stress cycles to failure at the constant amplitude stress range (S), and A and m are both material parameters. Estimation of the fatigue damage under random loading is assumed to follow the cumulative damage Miner method. In this method it is assumed the damage per load cycle is equal to the inverse number of cycles tolerated under the stress range (Tabias and Foutch, 1997; Kwon and Frangopol, 2010; Chryssanthopoulos and Righiniotis, 2006; Ayala-Uraga and Moan, 2007). So if the stress range S_i is identified in *i*-th cycle, the damage (D_i) is equal to:

$$D_i = \frac{1}{N_{fi}} \tag{5}$$

In which, N_{fi} is the number of cycles to failure at stress range S_i. In this formulation assumed the cumulative damage (D) is independent of the stress sequence so cumulative damage (D). Total damage accumulated over the time t is consequently equal to:

$$D = \sum_{i=1}^{n} \frac{1}{N_{fi}} = \sum_{i=1}^{n} \frac{S_i^m}{A} \tag{6}$$

Since the applied stress range is a random thus $\sum_{i=1}^{n} S_i^m$ would be also a random variable. If "n" becomes enough large, the uncertainty in the sum $\sum_{i=1}^{n} S_i^m$ will be too small (Bannantine et al. 1990) and consequently this summation can be substituted by its expected value and therefore:

$$E\left|\sum_{i=1}^{n} S_i^m\right| = E\,[n]\,E\left[S_i^m\right] \tag{7}$$

Thus, cumulative fatigue damage obtained from the following formula:

$$D = \frac{1}{A} E\,[n]\, E\left[S_i^m\right] \tag{8}$$

Well, failure occurs when the summation of D_i approaches to a critical value of Δ so the limit state function can be expressed by:

$$g(X,t) = \Delta - eD \tag{9}$$

Where "Δ" is the critical cumulative damage index and "e" is the error factor applicable in random loading. This random variable is covering the effect of any probable errors in estimating of the stress value. Substituting Equation (6) into (9) gives the limit state function as:

$$g(X,t) = \Delta - e\frac{n\,S_{re}^m}{A} \tag{10}$$

Various values have reported for the value of Δ. Based on the research reported by Wirsching (1995), if sufficient information is not available, lognormal distribution with mean value of 1 and coefficient of variation (COV) of 0.3 are reasonable for the steel metals (Kwon and Frangopol, 2010; Ayala-Uraga and Moan, 2007). A is a fatigue based coefficient contains all the uncertainty values in simulation. Therefore, its matching COV is assumed to be very large. In this article this value is obtained from the empirical data (Bannantine et al., 1990). In order to estimate fatigue life of the clips under variable stress range, the equivalent stress range is employed matching with Miner rule (Kwon and Frangopol, 2010). The equivalent stress rang is gained using the histogram by the following equation:

$$S_{re} = \left[\sum \frac{n_i}{N_{Total}} S_{ri}^m\right]^{\frac{1}{m}} \; or \; S_{re} = \left[\int_0^\infty S^m f_s(s) ds)\right]^{\frac{1}{m}} \tag{11}$$

In which, n_i is number of cycles in stress range of S_{ri} and N_{Total} is the number of total cycles. If $X_1 = \Delta$, $X_2 = A$ and $X_4 = S_{re}$ the limit state function can be expressed as:

$$g(X) = X_1 - n\frac{X_3 X_4^m}{X_2} \tag{12}$$

To calculate m and X_2, empirical data has been employed (Bannantine et al., 1990). The probability distribution, mean value and COV of random variables in Equation 12 have been listed in Table 5.

Table 5: Probability distribution of random variables with mean and coefficient of variation

Random variable	Probability Distribution	Mean (μ)	C.O.V
Miner's critical damage accumulation index(X_1)	Lognormal	1	0.30
Fatigue constant (X_2)	Lognormal	2.33e30 (MPa)	0.50
Error factor (X_3)	Lognormal	1	0.30
Equivalent stress range (X_4)	Lognormal	33.25 (MPa)	1.07
	Weibull	32.98 (MPa)	1.88

To determination of the reliability index, there are different approaches that can be used, including the FORM and Monte Carlo simulation (Nowak and Collins, 2000; Choi et al., 2007; Bannantine et al., 1990). First, variation of the reliability index against the operating time was obtained and a sensitivity analysis was performed to investigate influence of each random variable on the reliability index. To determine *n*the total load per year is assumed to be 12 million tons. The number of daily cycle is obtained based on passing the train with 20 wagons over the track. A computer program developed by using the MATLAB software to conduct reliability analysis of spring clips based on the FORM method. The graph Figure 11 shows the variation of reliability index versus the operating time. As can be seen, the reliability index of spring clips SKL14 was about 3 in first operation year. This was followed by a steady fall to 2.65 in 40 years of operation time. Based on survival probability of 95% a target reliability index is set to 1.65. Therefore the remaining life time of Vossloh spring clips estimated 100 years. It is note that a target reliability level may be determined based on the importance of track. In this research assumed the annual traffic rate was constant. So the variation of the annual traffic rate can effect on remaining life-time. To verify the result of the FORM technique, simultaneously the MCS method was also employed and the results of MSC approach were found to be well matched with the FORM technique.

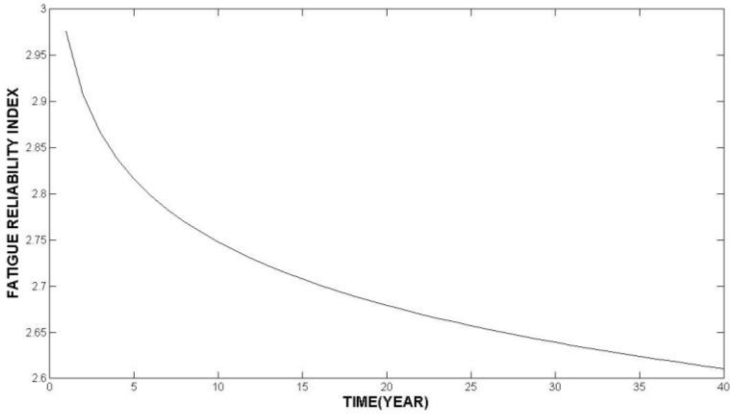

Figure 11: Fatigue reliability evaluation of Vossloh type SKL14

5 SENSITIVITY ANALYSIS

A sensitivity analysis was carried out to evaluate influences of the random variables on the reliability index. The effect of each random parameter on the reliability index has explained in Figure 12. As can see, the equivalent stress range (X4) had greatest impact rate (0.9). The second most effective variable was material parameter (A) with about 0.32 impact rate.

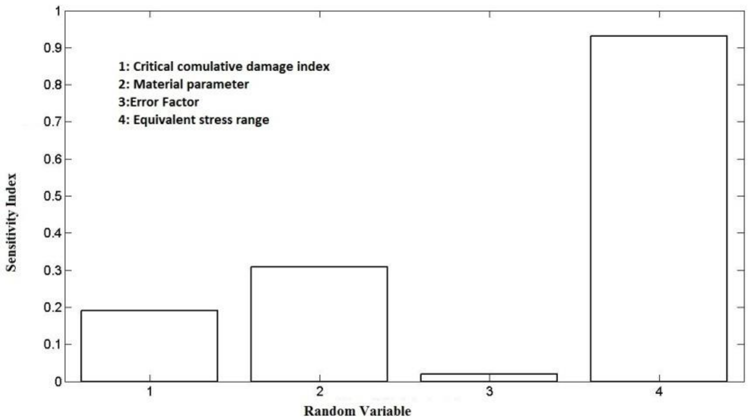

Figure 12: Sensitivity Analysis of random variables

Also the effect of daily cycle variation on reliability index was assessed. The daily cycle calculated based on simulated traffic in stations Arzhang-Andymeshk (Mohammadzadeh et al., 2012). Based on stress range bin histogram the mean value of equivalent stress range is calculated and the corresponding total number of cycles is considered as daily cycle. As shown in Figure 13 as increase of daily cycles 1827 to 23827, the reliability index decrease 5.50 to 4.30 in first year of lifetime. As can see, as daily cycle increased the reliability index curve in duration of 40 years move down. So with increase rate of traffic, the reliability index of SKL14 spring clips decreased.

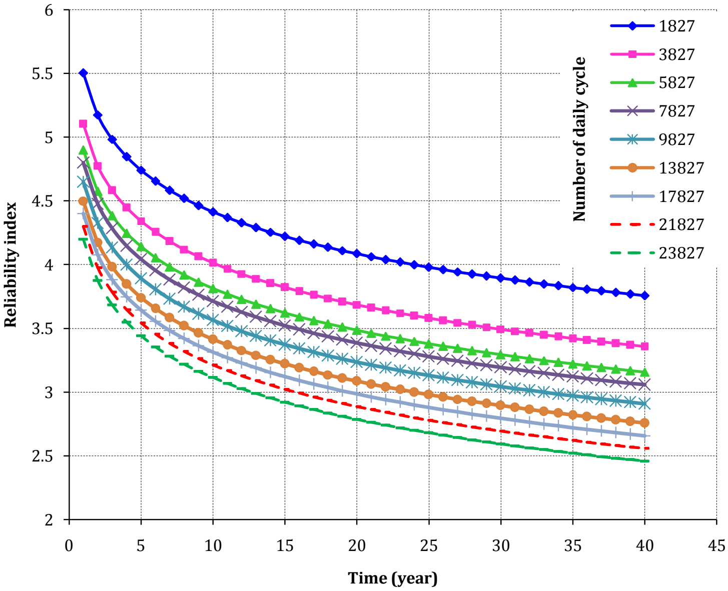

Figure 13: Effect of daily cycles on the reliability index during lifetime

The graph of Figure 14 shows the effect of changes of equivalent stress range on reliability index in duration lifetime of SKL14 spring clips. As can see, as the value of equivalent stress range varies 30 to 80MPa, the reliability index change 7 to 2 in first year of lifetime. Also as the equivalent stress range increase, the reliability index curve of 40 years go down.

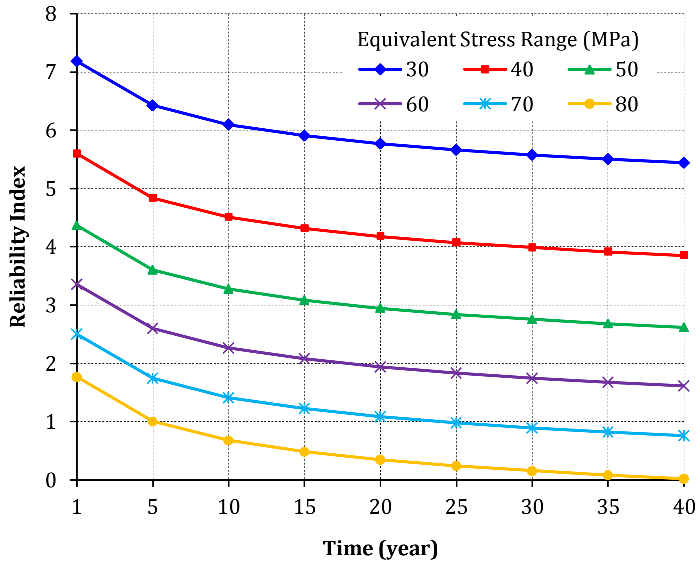

Figure 14: Effect of equivalent stress range on the reliability index during lifetime

6 CONCLUSION

A developed method for the fatigue reliability analysis of spring clips against random loading was conducted in this paper. This method can be extended for fatigue reliability analysis of similar ingredients of a railway tracks (for example: the rail pad, fastening bolts,) which subjected to random traffic loads. The proposed method was employed and the reliability of fatigue life of a typical SKL14 Vossloh spring clips was investigated. This model was developed for the random distribution of axle load as well as the operational speed based on empirical records. FEM of track and rail vehicle was developed and dynamic analysis was done under simulated traffic loads and time history of displacement of spring clips was gained. A reliable Finite Element model was constructed for the dynamic stress analysis of SKL14 and the stress concentrated regions as well as the critical dynamic stress values were recognized in spring clips. The main results can be listed as:

1- The equivalent stress range follows a lognormal distribution function.
2- It was found value of reliability index decreased from 3 to 2.6 for 40 years of operation and fatigue life of it can be expected as infinite.
3- Based on the conducted sensitivity analysis, between the four random variables, the equivalent stress range was proved to have the largest influence on the reliability index.
4- With increase of number of daily cycles from 1828 to 23828 the reliability index value drops from 5 to 4.30 in the first year of operation.
5- With increase of equivalent stress range from 30 to 80MPa, the reliability index decreases from 7 to 2 in the first year of operation.

References

Ayala-Uraga, E.,Moan, T. (2007). Fatigue reliability-based assessment of welded Joints applying consistent fracture mechanics formulation. International Journal of Fatigue 29(3):444-456.

Baecher, G. B., Christian, J. T. (2003). Reliability and statistics in geotechnical engineering.John Wiley &Sons, Inc.

Bannantine, J.A. Comer, J.J, Handrock, J.L. (1990). Fundamentals of metal fatigue analysis, Prentice Hall.

Bathe, K.J. (1996). Finite element procedures, Prentice Hall.

Choi, S.K., Grandhi, R.V., Canfield, R.A. (2007). Reliability-based structural design. Springer-Verlag London Limited.

Chotichai, P., Kanchanalal, T. (2006). Fatigue load spectra for steel railway bridges using simulation and field data. Symposium on Infrastructure Development and the Environment.

Chryssanthopoulos, M.K., Righiniotis, T.D. (2006). Fatigue reliability of welded steel structures. Journal of Constructional Steel Research 62(11):1199-1209.

Cremona, C., Lukic, M. (1998).Probability-based assessment and maintenance of welded joints damaged by fatigue. Nuclear Engineering and Design 182(3):253-266.

Cremona, C., Patron, A., Johansson, B., Larsson, T., Eichler, B., Höhler, S., Kühn, B. (2007). Improved assessment methods for static and fatigue resistance of old steel railway bridges, Background document D4.6, Sustainable Bridges.

Esveld, C. (2001). Modern Railway Track, MRT-production, Second edition, Netherland.

European standard, final draft prEN-13481 part 1~5 (2001). Railway application, track-performance requirements for fastening systems.

Farnaghi, M.R., Bahramivahdat, A. (2000). Acceptance standard for the spring clips type Vossloh.Iranian Railway Research Center.

Jianxi, W., Yude, X., Songliang, L., Liying, W. (2011). Probabilistic prediction model for initiation of RCF cracks in heavy-haul railway. International Journal of Fatigue 33:212-216.

Josefson, B.L., Ringsberg, J.W. (2009). Assessment of uncertainties in life prediction of fatigue initiation and propagation in welded rails. International Journal of Fatigue 31:1413-1421.

Kargarnovin, M.H., Younesian, D., Thompson, D.J., Jones, C.J.C. (2005). Ride comfort of high-speed trains travelling over railway bridges. Vehicle System Dynamics 43(3):173-197.

Kim, S.H., Lee, S.W., Mha, H.S. (2001). Fatigue reliability assessment of an existing steel railroad bridge.Engineering Structures 23:1203-1211.

Kwon, K., Frangopol, D.M. (2010). Bridge fatigue reliability assessment using probability density function of equivalent stress range based on field monitoring data. International Journal of Fatigue 32(8):1221-1232.

Lakusic, S., Bartos, D., Ante Goran, B. (2005). Experimental and numerical analysis of the rail fastening spring clips types SKL1- SKL12. Symposium on experimental methods in Solid Mechanics. 22nd DANUBIA-ADRIA Symposium on Experimental Methods in Solid Mechanics, Parma, University of Parma, 248-249.

Larsson, T. (2006). Material and Fatigue Properties of old metal Bridges, Licentiate Thesis, Lulea University of technology, Sweden.

Lee, O.S., Kim, D.H., Park, Y.C. (2008). Reliability of structures by using probability and fatigue theories. Journal of Mechanical Science and Technology 22(4):672-682.

Lichtberger, B. (2005). Track compendium: formation, permanent way, maintenance, economics. Eurail press, First edition.

Moghadam, A.S., Fallah, A. A., Mohammadzadeh, S. (2009). Reliability index for reinforced concrete frames using nonlinear pushover and dynamic analysis. International journal of advanced structural engineering 1(2):135-151.

Mohammadzadeh, S., Ghahremani, S. (2012).Estimation of train derailment probability using rail profile alterations.StructInfrastructEng 8(11):1034-1053.

Mohammadzadeh, S., Sangtarashha, M., Molatefi, H. (2011). A novel method to estimate derailment probability due to track geometric irregularities using reliability techniques and advanced simulation methods. Arch ApplMech 81(11):1621-1637.

Mohammadzadeh, S., Sharavi, M., Keshavarzian, H. (2013). Reliability analysis of fatigue crack initiation of railhead in bolted rail joint. Engineering Failure Analysis 29:132-148.

Mohammadzadeh, S., Shayanfar, M.A. (2004). Reliability analysis of railway bridges under the train dynamic loads using response surface method. 2nd International ASRANet Colloquium, Barcelona.

Mohammadzadeh, S., Vahabi.E. (2011). Time-dependent reliability analysis of B70 pre-stressed concrete sleeper subject to deterioration. Engineering Failure Analysis 18(1):421-432.

Newton, S.G., Clark, R.A. (1979). An investigation into the dynamic effects on the track of wheel flats on railway vehicles. Journal Mechanical Engineering Science 21(4):287-297.

NGI. Norwegian Geotechnical Institute. (2005). Final report :sustained performance of Railway tracks, Norway.

Nowak, A.S., Collins, K.R. (2000). Reliability of structures, McGraw-Hill.

Siddiqui, N.A., Ahmad, S. (2001). Fatigue and fracture reliability of TLP tethers under random loading. Marine Structures 14(3):331-352.

Stephens, R.I., Fatemi, A., Stephens, R.R., Fuchs, H.O. (2001).Metal fatigue in engineering.Second edition, John Wiley & Sons, Inc.

Sun, Y.Q., Dhanasekar, M. (2002).A dynamic model for the vertical interaction of the rail track and wagon system. International Journal of Solids and Structures 39:1337-1359.

Tabias, D.H, Foutch, D.A. (1997). Reliability-based method for fatigue evaluation of railway bridge. Journal of bridge engineering 2(2):53-60.

Wirsching P.H. (1995). "Probabilistic fatigue analysis".Probabilistic structural mechanics handbook, Sundararajan C, Springer-Science, 146-165.

Wysokowski, A. (2005). Simulation analysis of fatigue strength in steel highway bridges. Civil and Environmental Engineering Reports 1, University of Zielona Gora Press.

Xia, H., Xu, Y.L., Chan, T.H.T., Zakeri, J.A. (2007). Dynamic responses of railway Suspension bridges under moving trains.ScientiaIranica 14(5):385-394.

Younesian, D., Esmailzadeh, E., Mohammadzadeh, S. (2006). Dynamic performance, system identification and sensitivity analysis of ladder tracks. World Congress on Railway Research, Montreal, Canada.

Younesian, D., Kargarnovin, M.H. (2009). Response of the beams on random Pasternak foundations subjected to harmonic moving loads. Journal of Mechanical Science and Technology 23(11):3013-3023.

Younesian, D., Kargarnovin, M.H., Thompson, D.J., Jones, C.J.C. (2005). Parametrically excited vibration of a Timoshenko beam on viscoelastic foundation subjected to a harmonic moving load, Nonlinear Dynamics 45:75-93.

Zakeri, J.A., Xia, H. (2008). Sensitivity analysis of track parameters on train-track dynamic interaction. Journal of Mechanical Science and Technology 22(7):1299-1304.

Zakeri, J.A., Xia, H. (2009). Application of 2D-infinite beam elements in dynamic analysis of train-track interaction. Journal of Mechanical Science and Technology 23:1415-1421.

Zakeri, J.A., Xia, H., Fan, J.J. (2009). Dynamic responses of train-track system to single rail irregularity. Latin American Journal of Solids and Structures 6:89-104.

Zienkiewicz, O.C. (1977). The Finite Element Method, New York: McGraw-Hill Inc.

Appendix (A)

The overall differential equation of system (Figure 4) is represented by:

$$[M]\{\ddot{X}\}+[C]\{\dot{X}\}+[K]\{X\}=\{F(t)\}$$

Mass matrix: the mass matrixes of whole system and subsystem can be written as:

$$[M]=\begin{bmatrix}[M]_{Carbody\&Bogie\&Wheel} & & & \\ & [M]_{Rail} & & \\ & & [M]_{Sleeper} & \\ & & & [M]_{Ballast}\end{bmatrix}_{TDOF\times TDOF}$$

$$[M]_{Carbody\&Bogie\&Wheel}=diag(M_c,J_c,M_t,J_t,M_t,J_t,M_w,M_w,M_w,M_w)$$

$$[M]_{Sleeper}=diag(M_{s_1},M_{s_2},\ldots,M_{s_{NS}}) \qquad [M]_{Ballast}=diag(M_{b_1},M_{b_2},\ldots,M_{b_{NS}})$$

$$[M]_{Rail}=\sum_{i=1}^{NE}[M]^i_{Rail} \qquad [M]^i_{Rail}=\frac{m_rL_i}{420}\begin{bmatrix}156 & 22L_i & 54 & -13L_i \\ & 4L_i^2 & 13L_i & -3L_i^2 \\ & & 156 & -22L_i \\ sy. & & & 4L_i^2\end{bmatrix}$$

In above matrixes the word "diag" means diagonal matrix and all of mass matrixes are diagonal expect mass matrix of rail.

Stiffness matrix: the stiffness matrixes of system and component are written as:

$$[K]=\begin{bmatrix}[K]_{Carbody\&Bogie} & [K]_{C\&B/W} & & & \\ [K]_{W/C\&B} & [K]_{Wheel} & [K]_{W/R} & & \\ & [K]_{R/W} & [K]_{Rail} & [K]_{R/S} & \\ & & [K]_{S/R} & [K]_{Sleeper} & [K]_{S/B} \\ & & & [K]_{B/S} & [K]_{Ballast}\end{bmatrix}_{TDOF\times TDOF}$$

$$[K]_{Carbody\&Bogie}=\begin{bmatrix}2k_t & 0 & -k_t & 0 & -k_t & 0 \\ & 2k_tL_c^2 & -k_tL_c & 0 & k_tL_c & 0 \\ & & k_t+2k_w & 0 & 0 & 0 \\ & & & 2k_wL_t^2 & 0 & 0 \\ & & & & k_t+2k_w & 0 \\ & & & & & 2k_wL_t^2\end{bmatrix}$$

$$[K]_{C\&B/W} = \begin{bmatrix} 0 & 0 & 0 & 0 \\ 0 & 0 & 0 & 0 \\ -k_w & -k_w & 0 & 0 \\ -k_w L_t & k_w L_t & 0 & 0 \\ 0 & 0 & -k_w & -k_w \\ 0 & 0 & -k_w L_t & k_w L_t \end{bmatrix}$$

$$[K]_{Wheel} = diag(k_w, k_w, k_w, k_w) + diag(I_{w_1} k_H, I_{w_2} k_H, I_{w_3} k_H, I_{w_4} k_H)$$

$$I_{w_j} = \begin{cases} 1 & if \;\; X_{x_j} + R_{x_j} - X_{w_j} > 0 \\ 0 & else \end{cases}$$

$$[K]_{Sleeper} = diag(k_{b_1} + k_{p_1}, k_{b_2} + k_{p_2}, ..., k_{b_{NS}} + k_{p_{NS}}) \quad [K]_{Ballast} = diag(k_{b_1} + k_{f_1}, k_{b_2} + k_{f_2}, ..., k_{b_{NS}} + k_{f_{NS}})$$

$$K_{S/R} = \begin{bmatrix} -k_{p_1} & 0 & & & & & & & \\ 0 & 0 & -k_{p_2} & 0 & & & & & \\ & & 0 & 0 & \ddots & & & & \\ & & & & & -k_{p_{NS-1}} & 0 & 0 & 0 \\ & & & & & 0 & 0 & -k_{p_{NS}} & 0 \end{bmatrix}_{NS \times 2NJ}$$

$$K_{Ballast} = \begin{bmatrix} k_{b_1} + k_f + k_{sh} & -k_{sh} & 0 & & 0 \\ -k_{sh} & k_{b_2} + k_f + 2k_{sh} & -k_{sh} & & \\ & & \ddots & & \\ & & -k_{sh} & k_{b_{NS-1}} + k_f + 2k_{sh} & -k_{sh} \\ 0 & & & -k_{sh} & k_{b_{NS}} + k_f + k_{sh} \end{bmatrix}_{NS \times NS}$$

$$K_{S/B} = K_{B/S} = \begin{bmatrix} -k_{b_1} & 0 & & & 0 \\ 0 & \ddots & & & \\ & & -k_{b_i} & & \\ & & & \ddots & 0 \\ 0 & & & 0 & -k_{b_{NS}} \end{bmatrix}_{NS \times NS}$$

$$[K]_{Rail} = \sum_{i=1}^{NE} [K]^i_{Rail} \qquad [K]^i_{Rail} = \frac{EI}{L_i^3} \begin{bmatrix} 12 & 6L_i & -12 & 6L_i \\ & 4L_i^2 & -6L_i & 2L_i^2 \\ & & 12 & -6L_i \\ sy. & & & 4L_i^2 \end{bmatrix}$$

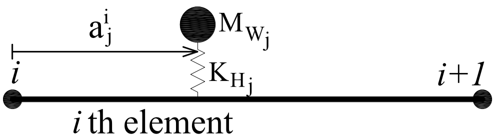

Figure 1A: The position of wheel between *i* and *i+1*

The matrixes of $[K_{Rail}]$، $[K_{W/R}]$ $[K_{R/W}]$ are changed in every time step based on position Figure 1A.
Damping matrix: the matrixes of system and subsystem are written as stiffness matrixes expect rail damping matrix.

$$[C]=\begin{bmatrix} [C]_{Carbody\&Bogie} & [C]_{C\&B/W} & & & \\ [C]_{W/C\&B} & [C]_{Wheel} & & & \\ & & [C]_{Rail} & [C]_{R/S} & \\ & & [C]_{S/R} & [C]_{Sleeper} & [C]_{S/B} \\ & & & [C]_{B/S} & [C]_{Ballast} \end{bmatrix}_{TDOF\times TDOF}$$

The damping matrix of rail calculated as:

$$[C]_{Rail}=\alpha[M]_{Rail}+\beta[K]_{Rail}$$

Forces matrixes: this matrix includes applied force on vehicle, rail, sleeper and ballast.

$$\{F(t)\}=\begin{Bmatrix} \{F_{Wagon}(t)\}_{10\times1} \\ \{F_{Rail}(t)\}_{2NJ\times1} \\ \{0\}_{2NS\times1} \end{Bmatrix}\quad \{F_{Wagon}(t)\}=\begin{Bmatrix} -M_c g \\ 0 \\ -M_b g \\ 0 \\ -M_b g \\ 0 \\ -M_w g \\ -M_w g \\ -M_w g \\ -M_w g \end{Bmatrix}+\begin{Bmatrix} 0 \\ 0 \\ 0 \\ 0 \\ 0 \\ 0 \\ K_{H_1}R_{x_1} \\ K_{H_2}R_{x_2} \\ K_{H_3}R_{x_3} \\ K_{H_4}R_{x_4} \end{Bmatrix}$$

$$\{F_{Rail}(t)\}_j^i=-k_{H_j}IR(a_j^i)\begin{bmatrix} -\varphi_1(a_j^i) \\ -\varphi_2(a_j^i) \\ -\varphi_3(a_j^i) \\ -\varphi_4(a_j^i) \end{bmatrix}\qquad \{F_{Rail}\}=\sum_{j=1}^{NW}\sum_{i=1}^{NE}\{F_{Rail}\}_j^i$$

$$F_{Contact_j}=C_{H_j}(X_{x_j}+R_{x_j}-X_{w_j})^{3/2}=$$
$$\left(C_{H_j}(X_{x_j}+R_{x_j}-X_{w_j})^{1/2}\right)(X_{x_j}+R_{x_j}-X_{w_j})=K_{H_j}(X_{x_j}+R_{x_j}-X_{w_j})$$

$K_{Hj}$is represents linear stiffness of Hertzian spring.